



Pseudovitelliform maculopathy associated with hereditary hemochromatosis

Ante Vukojevic ¹, Marija Vukojevic ², Tomislav Jukic ³, Igor Petricek ⁴, Kresimir Mandic ⁴ and Nenad Vukojevic ³

¹ Department of Ophthalmology, UHC Sestre Milosrdnice, Zagreb, Croatia

² Department of Emergency Medicine, County Institute of Emergency Medicine Sisak-Moslavina County, Sisak, Croatia

³ Department of Ophthalmology, School of Medicine, University of Zagreb, UHC Zagreb, Zagreb, Croatia

⁴ Department of Ophthalmology, UHC Zagreb, Zagreb, Croatia

ABSTRACT

Background: Hereditary hemochromatosis (HH) is an inherited autosomal recessive iron metabolism disorder resulting from a C282Y mutation in the *HFE* gene. Mutations in the *HFE* gene may result in iron accumulation and oxidative stress in the retina, resulting in macular degeneration. This article describes two patients with HH who were treated with erythrocytapheresis or phlebotomy, with no exposure to deferoxamine or any other chelation therapy, and who developed visual symptoms.

Case Presentation: Both patients had known diagnoses of HH. Because of visual symptoms, they were referred to the ophthalmology clinic and underwent a retinal exam, multimodal imaging, and electrodiagnostic studies, which revealed structural and functional degeneration of the central macula. Fundus photography, fluorescein angiography, and fundus autofluorescence revealed changes at the level of the retinal pigment epithelium (RPE) in the central macula. In addition, optical coherence tomography revealed subfoveal accumulation of hyperreflective material at and below the RPE. Multifocal electroretinography confirmed a decreased cone response, whereas the full-field electroretinogram was unremarkable. Genetic testing ruled out Best's vitelliform macular dystrophy and the other known hereditary macular dystrophies. The patients had known diagnoses of HH, homozygous C282Y mutations in the *HFE* gene, and no comorbidities; thus, we presumed that HH led to the observed morphological and functional disorders of the RPE, which in turn caused structural macular changes in both patients.

Conclusions: Considering the macular findings and the nature of the patients' primary illness, we believe that the accumulation of iron and photoreceptor metabolic products caused dysfunction in the RPE, which led to morphological and functional changes in the macula. Because the patients were not treated using chelating agents, we attribute the macular changes solely to iron accumulation and oxidative stress caused by the pathophysiological processes of HH. Further studies are needed to identify the plausible molecular or cellular insults underlying pseudovitelliform macular degeneration in patients with HH.

KEYWORDS


hereditary haemochromatosis protein precursor, human, haemochromatosis, mutations, overload, iron, pseudovitelliform, macula luteas, electroretinographies, electrooculograms, visual field test

Correspondence: Ante Vukojevic, Department of Ophthalmology, UHC Sestre Milosrdnice, Zagreb, Croatia. Email: ante.vukojevic1@gmail.com. ORCID iD: <https://orcid.org/0000-0002-0718-4135>

How to cite this article: Vukojevic A, Vukojevic M, Jukic T, Petricek I, Mandic K, Vukojevic N. Pseudovitelliform maculopathy associated with hereditary hemochromatosis. *Med Hypothesis Discov Innov Ophthalmol*. 2023 Winter; 12(4): 203-212. <https://doi.org/10.51329/mehdiophthal1487>

Received: 11 December 2023; Accepted: 30 January 2024



Copyright © Author(s). This is an open-access article distributed under the terms of the Creative Commons Attribution-NonCommercial 4.0 International License (<https://creativecommons.org/licenses/by-nc/4.0/>) which permits copy and redistribute the material just in noncommercial usages, provided the original work is properly cited. 

INTRODUCTION

Hereditary hemochromatosis (HH) is the most common hereditary disorder of iron metabolism [1]. It is an autosomal recessive disorder caused by a mutation of the *HFE* gene, which is found in the short arm of chromosome 6. The C282Y mutation is the most common mutation linked to hemochromatosis and occurs in 90% of diagnosed patients of northern European origin [1, 2]. The disorder is characterized by increased absorption of iron due to a disordered expression of hepcidin, which is the main regulator of iron homeostasis. Hepcidin expression is controlled by the free HFE protein (not bound to transferrin receptor 1 [TfR1]), which upregulates hepcidin expression. If the binding of HFE proteins to TfR1 increases, the signal is interrupted and hepcidin expression decreases [3]. A reduction in hepcidin expression leads to progressive accumulation of iron in cells and tissues, ultimately causing organ dysfunction [4].

Patients experiencing secondary iron overload are known to have changes in the retina. However, these changes are caused by the toxicity of deferoxamine mesylate, which, on account of its chelating characteristics, is used to eliminate excess iron [5, 6]. Patients treated with deferoxamine have developed several disorders such as retinopathy, bull's eye maculopathy, and vitelliform maculopathies [5, 6]. Importantly, the morphological changes in the retina are not only related to deferoxamine mesylate toxicity, but can also result from iron deposition in secondary hemochromatosis and in the pathophysiological processes of HH that has not been treated with chelating agents [7]. The importance of the *HFE* gene in regulating retinal iron homeostasis was previously described, and a knockout mouse model has shown that iron accumulation may have destructive effects on the retinal pigment epithelium (RPE), causing oxidative stress and damage [8, 9].

This article describes the structural macular changes in two patients with diagnoses of HH caused by the C282Y mutation of the *HFE* gene. Both patients were treated with erythrocytapheresis or phlebotomy, were not exposed to deferoxamine or any other chelation therapy, and had no pre-existing genetically confirmed diagnoses of known inherited retinal dystrophies.

CASE PRESENTATION

Patient 1

A 63-year-old man presented to the ophthalmology department because of blurred vision and diplopia, for which he has been monitored. For the prior 11 years, he had been monitored for a diagnosis of HH with a homozygous C282Y mutation of the *HFE* gene. Figure 1 displays the pedigree [10] of the patient. The patient

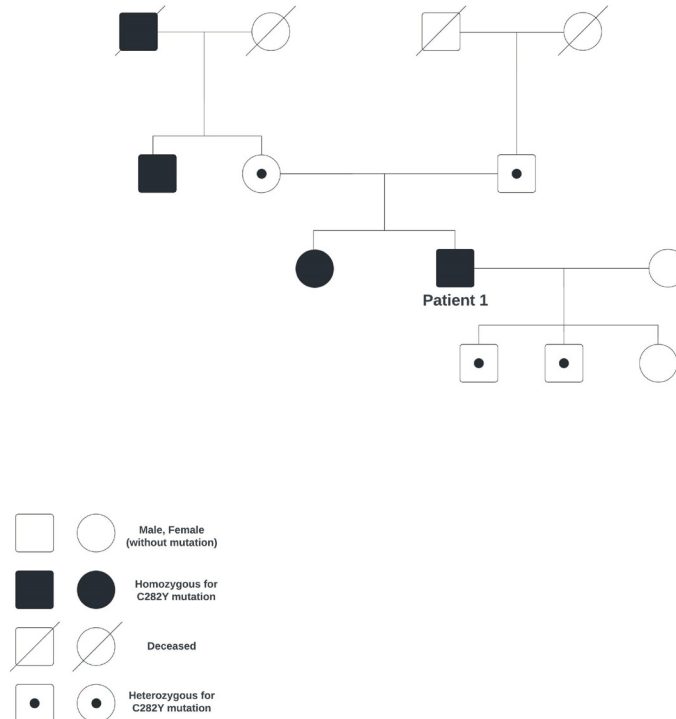


Figure 1. Pedigree of patient 1.

underwent examinations by a cardiologist [11], endocrinologist [12], and gastroenterologist [13], all of whom excluded the presence of cardiomyopathic diseases and diabetes. Since then, whole-blood phlebotomy [14, 15] had been performed every three months, along with monitoring of blood cell counts and ferritin levels.

A biochemical assessment [16] during the ophthalmological workup revealed a serum ferritin concentration of 159 $\mu\text{g/L}$ (reference range: 20 – 250 $\mu\text{g/L}$), whereas the serum iron concentration was 19 $\mu\text{mol/L}$ (reference range: 8 – 30 $\mu\text{mol/L}$) and the unsaturated iron binding capacity was 30 $\mu\text{mol/L}$ (reference range: 26 – 59 $\mu\text{mol/L}$).

During the first ophthalmological evaluation, the best corrected distance visual acuity (BCDVA) using a Snellen chart (CC-100XP LED LCD Chart; Topcon Corp., Tokyo, Japan) was 1.0 in the right eye and 1.0 in the left eye in decimal notation [17]. A detailed ocular examination using a slit lamp (Topcon SL-D301; Topcon Corp.) revealed only an incipient cataract on the posterior pole of the left crystalline lens. Intraocular pressure measured using a Goldmann applanation tonometer (AT900; Haag-Streit, Koeniz, Switzerland) was within normal limits in both eyes. Fundus examination using a slit lamp (Topcon SL-D301; Topcon Corp.) with a 78 diopter lens (Volk Optical Inc., Mentor, OH, USA) revealed a yellowish lesion at the center of each macula, measuring $< \frac{1}{4}$ disc diameter in greatest dimension, with distinct and well-defined margins (Figure 2A, B). Fundus autofluorescence (VISUCAMNM/FA; Carl Zeiss Meditec AG, Jena, Germany) showed autofluorescent lesions in the corresponding areas (Figure 2C, D), whereas fluorescein fundus angiography (VISUCAM NM/FA; Carl Zeiss Meditec AG) showed early hyperfluorescence in the foveas due to window defects and minor hypofluorescence without evidence of leakage (Figure 2E, F).

Optical coherence tomography (OCT) (Copernicus HR-SOCT; Optopol Technology SA, Zawiercie, Poland) revealed subfoveal, oval, and dense deposits and disruption of the ellipsoid zone and external

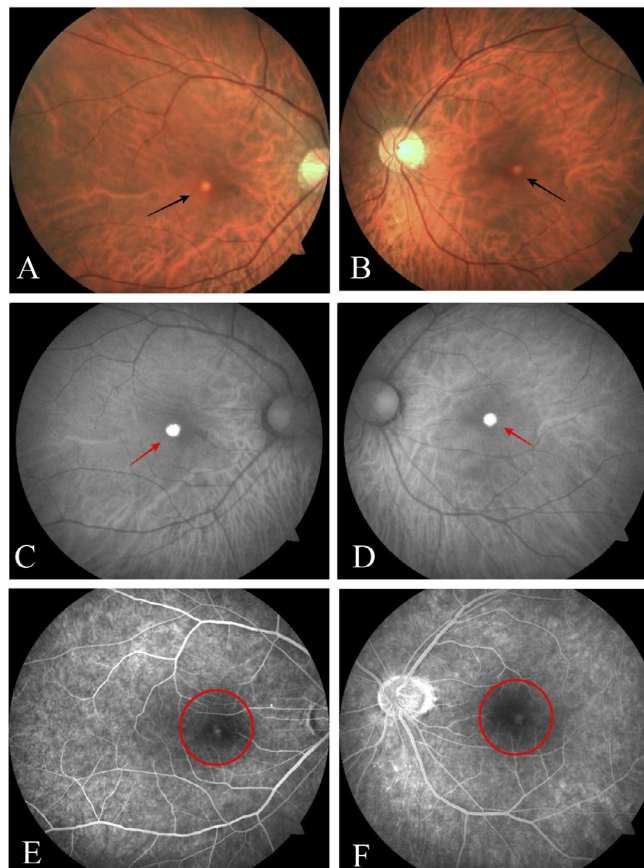


Figure 2. Fundus photographs (VISUCAM NM/FA; Carl Zeiss Meditec AG, Jena, Germany) of the right (A) and left (B) eyes revealed a depigmented yellow lesion (black arrows) in each macula, measuring $< \frac{1}{4}$ disc diameter in greatest dimension, with distinct and well-defined margins. Fundus autofluorescence (VISUCAM NM/FA; Carl Zeiss Meditec AG) revealed an oval subretinal autofluorescent deposit presenting as a single lesion (red arrows) in the central macula of the right (C) and left (D) eyes. Fluorescein fundus angiography (VISUCAM NM/FA; Carl Zeiss Meditec AG) revealed early hyperfluorescence in the corresponding areas due to window defects and minor hypofluorescence without evidence of leakage in the right (E) and left (F) eyes (red circles).

limiting membrane (Figure 3A, B). A full-field electroretinogram (Ganzfeld Q450; Roland Consult Stasche & Finger GmbH, Brandenburg/Havel, Germany) revealed a normal retinal response. An electrooculogram (Ganzfeld Q450; Roland Consult Stasche & Finger GmbH) revealed a reduced Arden ratio of 3/2.5 [18]. A multifocal electroretinogram (Ganzfeld Q450; Roland Consult Stasche & Finger GmbH) revealed diffuse and emphasized amplitude reduction in the P1 waves for both eyes (Figure 3C, D). The visual field (Manual Goldmann Perimeter 940; Haag-Streit) was slightly concentrically narrowed in both eyes (Figure 3E, F).

The patient underwent clinical exome sequencing using the Trusight One sequencing panel (Illumina, San Diego, CA, USA) on the NextSeq 550 sequencing platform (Illumina). Homozygous p.C282Y mutations in the *HFE* gene were detected. The Trusight One sequencing panel [19] consists of 4800 genes. Among these are genes related to the most common known macular dystrophies according to the HP term macular dystrophy (HP:0007754). No pathogenic or uncertain significance (VUS) [19] variants were detected after filtering for macular dystrophy genes. Throughout five years of ophthalmological monitoring, the patient's BCDVA remained stable and the macular lesions remained unchanged.

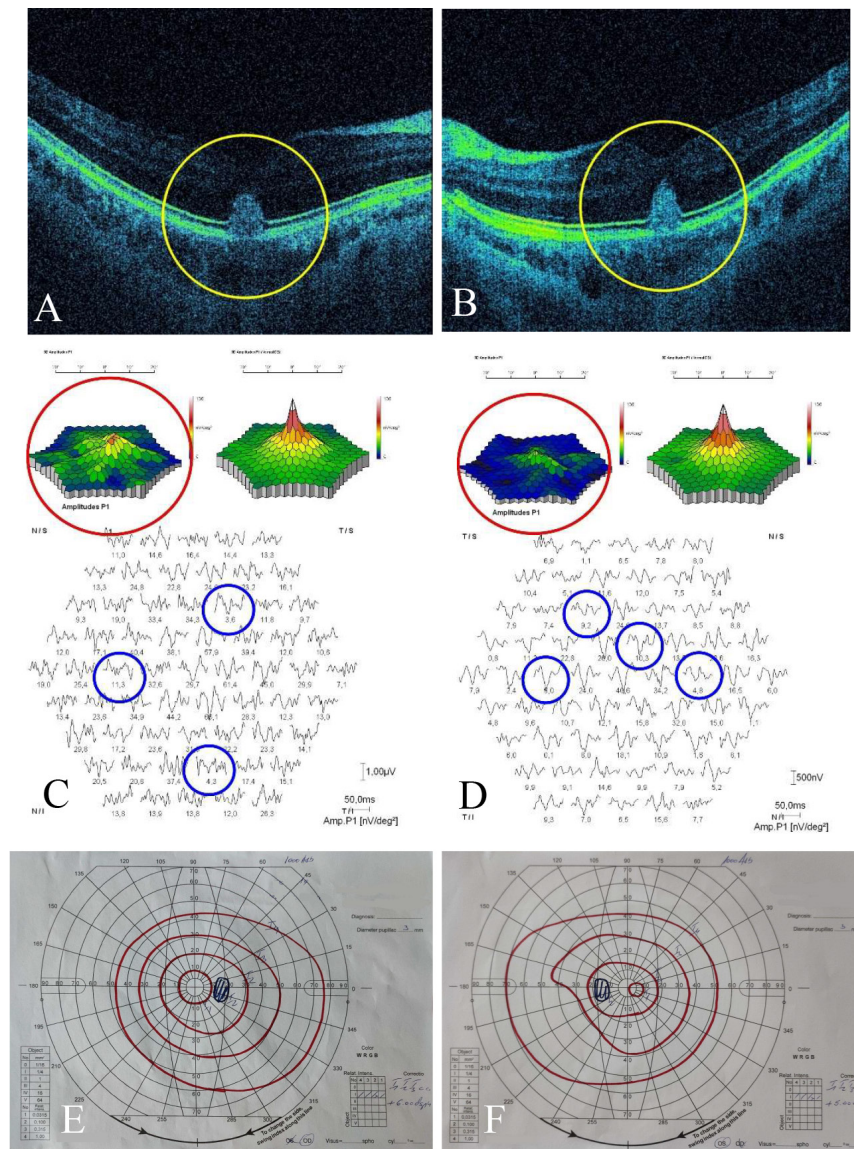


Figure 3. Optical coherence tomography (Copernicus HR-SOCT; Optopol Technology SA, Zawiercie, Poland) revealed a subfoveal, hyperreflective lesion (yellow circles) in the outer layers of the macula in the right (A) and left (B) eyes. A multifocal electroretinogram (Ganzfeld Q450; Roland Consult Stasche & Finger GmbH, Brandenburg/Havel, Germany) revealed diffuse and emphasized amplitude reduction in the P1 waves (blue circles) and emphasized reduction of the cone response (red circles) in the macula of both the right (C) and left (D) eyes. A slightly concentrically narrowed visual field (Manual Goldmann Perimeter 940; Haag-Streit, Koeniz, Switzerland) was detected in the right (E) and left (F) eyes.

Patient 2

A 47-year-old man presented to the ophthalmology department because of visual symptoms in the form of a central dark spot in the visual field of the right eye. The patient had been monitored for dizziness by a neurologist, who recommended magnetic resonance imaging of the brain, the results of which were unremarkable. The patient was examined at the hematology department because of elevated serum concentrations of ferritin and iron. A biochemical assessment [16] during the ophthalmological workup revealed a serum ferritin concentration of 962.8 µg/L (reference range: 20 – 250 µg/L), whereas serum iron concentration was 25 µmol/L (reference range: 8 – 30 µmol/L) and the unsaturated iron binding capacity was 22 µmol/L (reference range: 26 – 59 µmol/L).

Before presenting to the ophthalmology clinic, HH (homozygous C282Y mutation) had been diagnosed, for which the patient underwent erythrocytapheresis every three months [15]. Figure 4 displays the pedigree [10] of the patient. The patient underwent examinations by a cardiologist [11], endocrinologist [12], and gastroenterologist [13], all of whom excluded the presence of cardiomyopathic diseases and diabetes.

The ophthalmological assessment revealed a decrease in BCDVA in both eyes. The BCDVA evaluated using a Snellen chart (CC-100XP LED LCD Chart; Topcon Corp.) was 0.8 in the right eye and 0.7 in the left eye in decimal notation [17]. A detailed slit-lamp examination (Topcon SL-D301, Topcon Corp.) revealed normal anterior segments. Intraocular pressure measured using a Goldmann applanation tonometer (AT900; Haag-Streit) was normal in both eyes. Fundus examination using a slit lamp (Topcon SL-D301; Topcon Corp.) with a 78 diopter lens (Volk Optical, Inc.) revealed a small, round, yellowish lesion at the center of each macula, the largest measuring $< \frac{1}{4}$ disc diameter, with distinct and well-defined margins, along with RPE changes in the right macula (Figure 5A, B). Fundus autofluorescence (VISUCAM NM/FA; Carl Zeiss Meditec AG) revealed oval autofluorescent lesions in the corresponding areas (Figure 5C, D), whereas fluorescein fundus angiography (VISUCAM NM/FA; Carl Zeiss Meditec AG) revealed a hypofluorescent blocking lesion in the central macula, surrounded by a narrow zone of early hyperfluorescence due to window defects without evidence of leakage (Figure 5E, F).

OCT (Copernicus HR-SOCT; Optopol Technology SA) revealed subfoveal disorders of the RPE, a disruption of the ellipsoid zone and external limiting membrane, and deposits in the outer layers of the macula

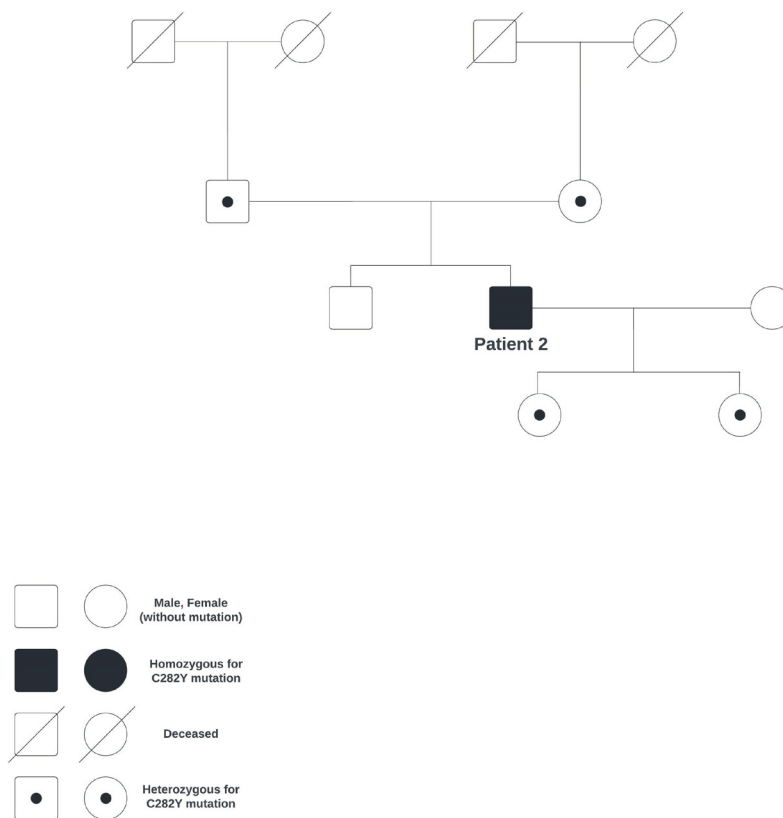


Figure 4. Pedigree of patient 2.

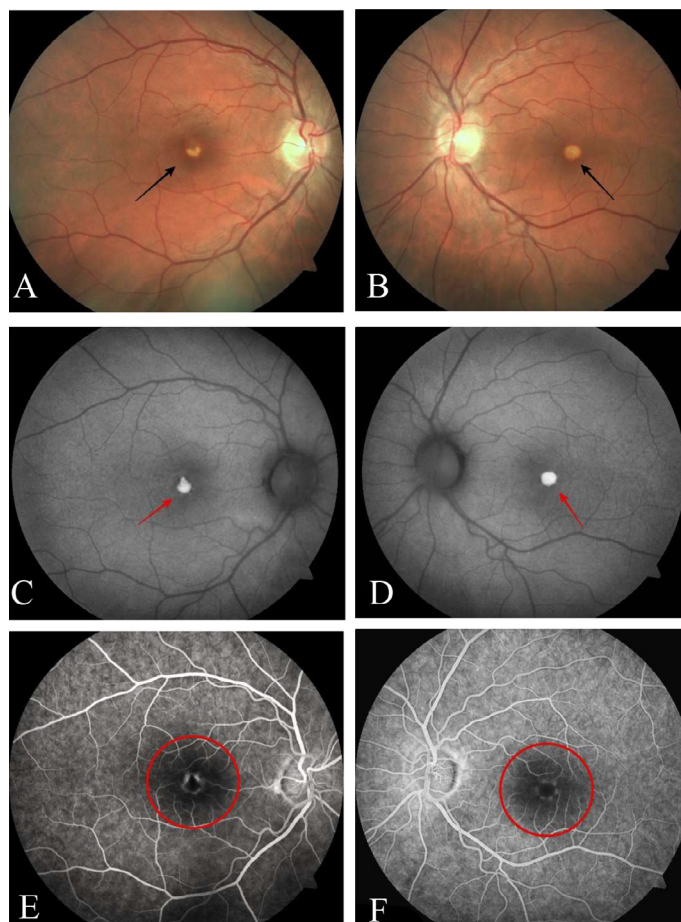


Figure 5. Fundus photography (VISUCAM NM/FA; Carl Zeiss Meditec AG, Jena, Germany) of the right (A) and left (B) eyes revealed a depigmented yellow lesion (black arrows) in each macula, the largest measuring $< \frac{1}{4}$ disc diameter, with distinct and well-defined margins, along with the retinal pigment epithelium changes in the right macula. Fundus autofluorescence (VISUCAM NM/FA; Carl Zeiss Meditec AG) revealed partially depigmented subretinal autofluorescent deposits presenting as a single macular lesion (red arrows) in the central macula of the right (C) and left (D) eyes. Fluorescein fundus angiography (VISUCAM NM/FA; Carl Zeiss Meditec AG) revealed early hyperfluorescence in the peripheral part of the lesion due to window defects without evidence of leakage, along with blockage in the center of the lesion due to pigment accumulation (clumping) in the right (E) and left (F) eyes (red circles).

(Figure 6A, B). A full-field electroretinogram (Ganzfeld Q450; Roland Consult Stasche & Finger GmbH) revealed a normal retinal response, and an electrooculogram (Ganzfeld Q450; Roland Consult Stasche & Finger GmbH) revealed a reduced Arden ratio of 2.1/2.3 [18]. Despite foveal structural changes, a multifocal electroretinogram (Ganzfeld Q450; Roland Consult Stasche & Finger GmbH) showed the amplitude of P1 waves to be within normal limits in both eyes (Figure 6C, D). The visual field (Manual Goldmann Perimeter 940; Haag-Streit) was slightly concentrically narrowed in both eyes (Figure 6E, F).

The patient underwent clinical exome sequencing using the Trusight One sequencing panel (Illumina) on the Nextseq 550 sequencing platform (Illumina). Homozygous p.C282Y mutations in the *HFE* gene were detected. The Trusight One sequencing panel [19] consists of 4800 genes. Among these are genes related to the most common known macular dystrophies according to the HP term macular dystrophy (HP:0007754). No pathogenic or VUS variants [19] were detected after filtering for macular dystrophy genes. Throughout three years of monitoring in the ophthalmology clinic, BCDVA has remained stable, and the macular lesions have remained unchanged.

This study was conducted in accordance with the Declaration of Helsinki and was approved by the Ethics Committee of the University Hospital Center Zagreb (02/21-JG [Class: 8. 1-21/85-2]). Written informed consent was obtained from both patients for publication of this material.

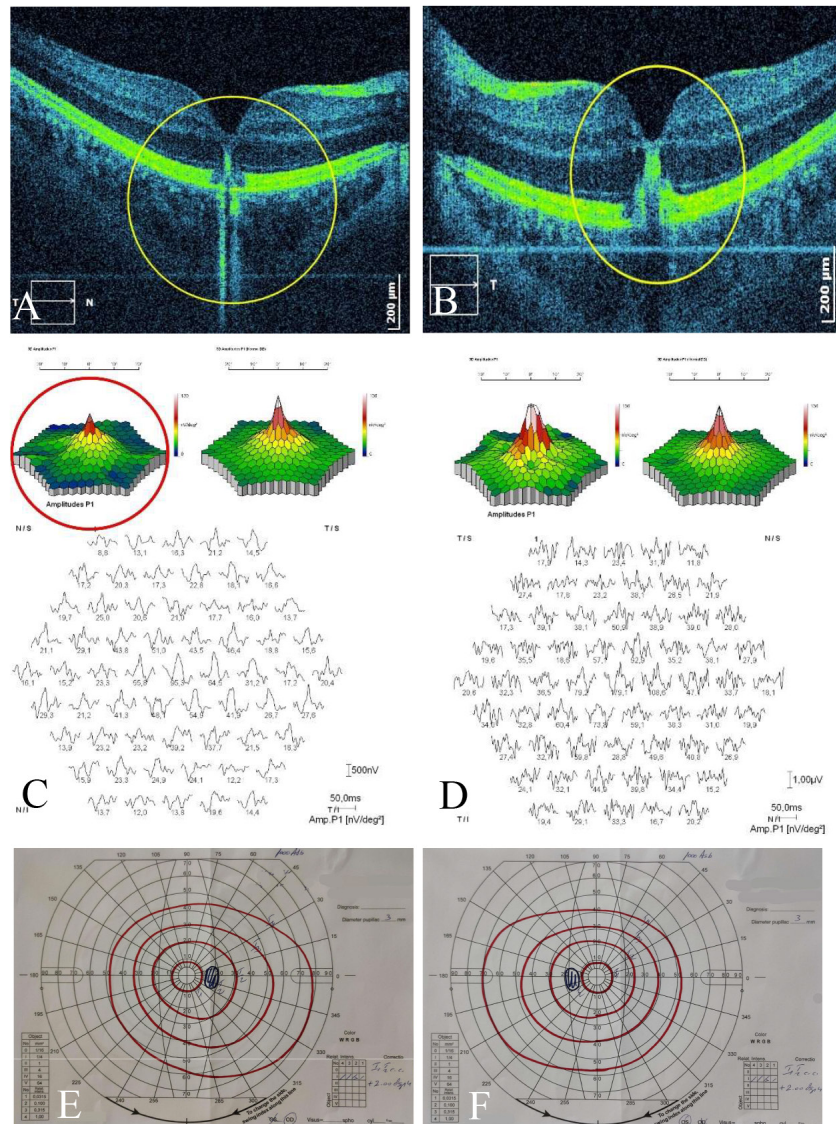


Figure 6. Optical coherence tomography (Copernicus HR-SOCT; Optopol Technology SA, Zawiercie, Poland) revealed damage to the retinal pigment epithelium, deposits of hyperreflective material, and pigment migration toward the inner layers of the macula of the right (A) and left (B) eyes. A multifocal electroretinogram (Ganzfeld Q450; Roland Consult Stasche & Finger GmbH, Brandenburg/Havel, Germany) revealed the amplitude of P1 waves to be within physiological limits for both eyes and a discrete reduction of cone response more to the periphery (red circle) in the right eye (C), and a normal cone response in the left eye (D). A slightly concentrically narrowed visual field (Manual Goldmann Perimeter 940; Haag-Streit, Koeniz, Switzerland) was found for both the right (E) and left (F) eyes.

DISCUSSION

We have presented two patients with visual symptoms, manifesting as blurred vision and diplopia in the first patient and a dark spot in the central visual field in the second patient. They underwent clinical examinations involving multimodal imaging and electrodiagnostic studies, which confirmed pseudovitelliform macular degeneration in the central macula for both. Clinical exome sequencing ruled out Best's disease and other known hereditary macular dystrophies. The patients had known diagnoses of HH, homozygous C282Y mutations in the *HFE* gene, and no comorbidities; thus, we presumed that HH led to the observed morphological and functional disorders of the RPE, which in turn caused structural macular changes in both patients.

Iron has an important function in the RPE, primarily as a cofactor of the RPE65 protein. This protein is important for retinoid metabolism [20], the activity of guanylate cyclase in the synthesis of cyclic guanosine monophosphate in phototransduction, the activity of fatty acid desaturase in synthesizing lipids for new disk membranes in the outer segments of photoreceptors, their phagocytosis, and the lysosomal activities of the

RPE [20, 21], thereby ensuring photo-excitability [8]. Moreover, iron is crucial for the functioning of several enzymes responsible for neurotransmitter homeostasis [20]. Therefore, disorders of iron metabolism may lead to pathological functions and morphological changes in the retina. This could explain the clinical and paraclinical changes that we observed in our patients.

In HH with mutations of the *HFE* gene, there is disordered expression of the HFE protein, which is predominantly found on the basolateral side of the RPE, and there, binding to TfR1 and TfR2, it participates in controlling metabolism and iron homeostasis [8, 22]. Iron homeostasis disorder leads to a series of pathological changes. As in all tissues affected by hemochromatosis, iron overload occurs in eye tissues as well [23], as observed in the study with *Hfe*^{-/-} mice [8]. In addition to iron accumulation, hypertrophy and/or hyperplasia of the RPE also occur [9], which is not only inherent to pathological processes in HH but also in aceruloplasminemia with disorders of the ceruloplasmin ferroxidase enzyme [24] and in age-related macular degeneration [25]. Degenerative changes in these conditions could be attributed to iron overload, which leads to the production of highly reactive hydroxyl radicals through Fenton reactions, thus creating oxidative stress and damage [26]. These pathological processes could explain the macular changes in our patients.

The observed thickening in OCT may correspond to the accumulation of metabolic products and residual outer segments of photoreceptors, which are usually phagocytosed in the normal physiological state [27]. Outer segments of photoreceptors remain accumulated in the external layers of the retina due to dysfunction of phagocytosis and transport through the RPE. Damage to the RPE, evident as window defects on fluorescein fundus angiography (Figures 2E, F and 5E, F), could be attributed to iron overload in RPE cells and the intercellular spaces and degeneration of RPE cells, which could explain the other components of the macular lesions. Structural changes were also visible on OCT as disrupted continuity of the RPE and migration of RPE cells (Figures 3A, B and 6A, B).

In addition to the aforementioned structural alterations, functional modifications also confirmed the damage to the RPE. The Arden index for both patients was less than 1.5 [18], suggesting that the damage occurred at the RPE and possibly Bruch's membrane and the interstitial space between these two structures, as observed in Best's disease [28, 29]. Considering that genetic testing excluded Best's disease, iron overload may have played a substantial role in the pathophysiology associated with HH in our patients. We believe that the low Arden indexes in our patients could be due to several mechanisms such as iron overload [30], oxidation by oxygen free radicals, disruption of the RPE [31], or other undiscovered mechanisms.

In addition to the presence of oxidative effects of hydroxyl radicals, we believe that the duration of exposure to oxidative stress [32] is an essential factor in the development of morphological and functional changes in the retina. Morphological changes were described in 18-month-old *Hfe*^{-/-} mice, whereas in *Hfe*^{-/-} mice at 4, 8, and 12 weeks of age, no morphological changes were found [9]. This suggests that morphological changes increase with a longer duration of tissue exposure to oxidative stress. For the prior 11 years, our first patient had been monitored for a diagnosis of HH with a homozygous C282Y mutation of the *HFE* gene. Before presenting to the ophthalmology clinic, HH (homozygous C282Y mutation) had been diagnosed in the second patient, for which the patient underwent erythrocytapheresis every three months [15].

Functional changes in the retina could explain the conditions of our patients. Specifically, the 63-year-old patient with subjective blurring of vision exhibited a poorer response of the cones, along with diffusive and emphasized reduction of P1 wave amplitude in both eyes (Figure 3C, D), whereas the 47-year-old patient with a dark spot in the central visual field of the right eye showed a slightly reduced response of the peripheral cones with physiological amplitudes of P1 waves in both eyes (Figure 6C, D). The decreased amplitude of the P1 waves could indicate that iron toxicity and oxidative stress caused retinal dysfunction at the level of photoreceptors and bipolar cells [20]. Considering that the cones may be more sensitive to oxidative stress than other parts of the retina [33], the duration of exposure to oxidative stress may have great significance in the onset of morphological and functional changes to the retina.

Herein, we have reported two cases of pseudovitelliform macular degeneration in patients with genetically confirmed HH who were treated with erythrocytapheresis or phlebotomy but not with deferoxamine or any other chelation therapy. However, we were unable to determine the molecular or cellular nature of the pseudovitelliform appearance in the macula. Further studies using comparative animal models of human HH could provide compelling evidence for the involvement of our proposed mechanisms in the pathogenesis of the observed macular changes in these patients.

CONCLUSIONS

Ocular examinations of two patients with genetically confirmed HH revealed morphological and functional

changes in the macula. Because the patients were not treated using chelating agents, we attribute the macular changes solely to iron accumulation and oxidative stress caused by the pathophysiological processes of HH. In addition, further deterioration of macular function and morphology is expected owing to the duration of the primary disease. Further studies are needed to identify the plausible molecular or cellular insults underlying pseudoviteliform macular degeneration in patients with HH.

ETHICAL DECLARATIONS

Ethical approval: This study was conducted in accordance with the Declaration of Helsinki and was approved by the Ethics Committee of the University Hospital Center Zagreb (02/21-JG [Class: 8. 1-21/85-2]). Written informed consent was obtained from both patients for publication of this material.

Conflict of interests: None

FUNDING

None.

ACKNOWLEDGMENTS

This paper has been published previously as a preprint in preprints.org (doi: <https://doi.org/10.20944/preprints202306.1051.v1>, June 2023).

REFERENCES

- Geller SA, de Campos FP. Hereditary hemochromatosis. *Autops Case Rep.* 2015;5(1):7-10. doi: 10.4322/acr.2014.043 pmid: 26484318
- Distante S, Robson KJ, Graham-Campbell J, Arnaiz-Villena A, Brissot P, Worwood M. The origin and spread of the HFE-C282Y haemochromatosis mutation. *Hum Genet.* 2004;115(4):269-79. doi: 10.1007/s00439-004-1152-4 pmid: 15290237
- Frazer DM, Anderson GJ. The orchestration of body iron intake: how and where do enterocytes receive their cues? *Blood Cells Mol Dis.* 2003;30(3):288-97. doi: 10.1016/s1079-9796(03)00039-1 pmid: 12737947
- Pilling LC, Tamosauskaite J, Jones G, Wood AR, Jones L, Kuo CL, et al. Common conditions associated with hereditary haemochromatosis genetic variants: cohort study in UK Biobank. *BMJ.* 2019;364:k5222. doi: 10.1136/bmj.k5222. Erratum in: *BMJ.* 2019;367:l6157 pmid: 30651232
- Di Nicola M, Barteselli G, Dell'Arti L, Ratiglia R, Viola F. Functional and Structural Abnormalities in Deferoxamine Retinopathy: A Review of the Literature. *Biomed Res Int.* 2015;2015:249617. doi: 10.1155/2015/249617 pmid: 26167477
- Bayraktar Bilen N, Polat Gültekin B, Dagdas S, Kalayci D. Deferoxamine-related bilateral maculopathy with optical coherence tomography findings. *Photodiagnosis Photodyn Ther.* 2023;45:103961. doi: 10.1016/j.pdpdt.2023.103961 pmid: 38163453
- Bellsmith KN, Dunaief JL, Yang P, Pennesi ME, Davis E, Hofkamp H, et al. Bull's eye maculopathy associated with hereditary hemochromatosis. *Am J Ophthalmol Case Rep.* 2020;18:100674. doi: 10.1016/j.ajoc.2020.100674 pmid: 32258826
- Gnana-Prakasam JP, Martin PM, Smith SB, Ganapathy V. Expression and function of iron-regulatory proteins in retina. *IUBMB Life.* 2010;62(5):363-70. doi: 10.1002/iub.326 pmid: 20408179
- Gnana-Prakasam JP, Thangaraju M, Liu K, Ha Y, Martin PM, Smith SB, et al. Absence of iron-regulatory protein Hfe results in hyperproliferation of retinal pigment epithelium: role of cystine/glutamate exchanger. *Biochem J.* 2009;424(2):243-52. doi: 10.1042/BJ20090424 pmid: 19715555
- Bennett RL, French KS, Resta RG, Doyle DL. Standardized human pedigree nomenclature: update and assessment of the recommendations of the National Society of Genetic Counselors. *J Genet Couns.* 2008;17(5):424-33. doi: 10.1007/s10897-008-9169-9 pmid: 18792771
- Danilowicz-Szymanowicz L, Świątczak M, Sikorska K, Starzyński RR, Raczak A, Lipiński P. Pathogenesis, Diagnosis, and Clinical Implications of Hereditary Hemochromatosis-The Cardiologic Point of View. *Diagnostics (Basel).* 2021;11(7):1279. doi: 10.3390/diagnostics11071279 pmid: 34359361
- Pelusi C, Gasparini DI, Bianchi N, Pasquali R. Endocrine dysfunction in hereditary hemochromatosis. *J Endocrinol Invest.* 2016;39(8):837-47. doi: 10.1007/s40618-016-0451-7 pmid: 26951056
- Pietrangelo A. Hereditary hemochromatosis: pathogenesis, diagnosis, and treatment. *Gastroenterology.* 2010;139(2):393-408, 408.e1-2. doi: 10.1053/j.gastro.2010.06.013 pmid: 20542038
- Alexander J, Kowdley KV. HFE-associated hereditary hemochromatosis. *Genet Med.* 2009;11(5):307-13. doi: 10.1097/GIM.0b013e31819d30f2 pmid: 19444013
- Rombout-Sestrienkova E, Winkens B, Essers BA, Nieman FH, Noord PA, Janssen MC, et al. Erythrocytapheresis versus phlebotomy in the maintenance treatment of HFE hemochromatosis patients: results from a randomized crossover trial. *Transfusion.* 2016;56(1):261-70. doi: 10.1111/trf.13328 pmid: 26358375
- Chambers V, Sutherland L, Palmer K, Dalton A, Rigby AS, Sokol R, et al. Haemochromatosis-associated HFE genotypes in English blood donors: age-related frequency and biochemical expression. *J Hepatol.* 2003;39(6):925-31. doi: 10.1016/s0168-8278(03)00471-9 pmid: 14642607
- Williams MA, Moutray TN, Jackson AJ. Uniformity of visual acuity measures in published studies. *Invest Ophthalmol Vis Sci.* 2008;49(10):4321-7. doi: 10.1167/iov.07-0511 pmid: 18829857

18. Thavikulwat AT, Lopez P, Caruso RC, Jeffrey BG. The effects of gender and age on the range of the normal human electro-oculogram. *Doc Ophthalmol*. 2015;131(3):177-88. doi: [10.1007/s10633-015-9514-x](https://doi.org/10.1007/s10633-015-9514-x) pmid: 26474906
19. Di Resta C, Spiga I, Presi S, Merella S, Pipitone GB, Manitto MP, et al. Integration of multigene panels for the diagnosis of hereditary retinal disorders using Next Generation Sequencing and bioinformatics approaches. *EJIFCC*. 2018;29(1):15-25. pmid: 29765283
20. Shahandeh A, Bui BV, Finkelstein DI, Nguyen CTO. Effects of Excess Iron on the Retina: Insights From Clinical Cases and Animal Models of Iron Disorders. *Front Neurosci*. 2022;15:794809. doi: [10.3389/fnins.2021.794809](https://doi.org/10.3389/fnins.2021.794809) pmid: 35185447
21. Chen H, Lukas TJ, Du N, Suyeoka G, Neufeld AH. Dysfunction of the retinal pigment epithelium with age: increased iron decreases phagocytosis and lysosomal activity. *Invest Ophthalmol Vis Sci*. 2009;50(4):1895-902. doi: [10.1167/iops.08-2850](https://doi.org/10.1167/iops.08-2850) pmid: 19151392
22. Martin PM, Gnana-Prakasam JP, Roon P, Smith RG, Smith SB, Ganapathy V. Expression and polarized localization of the hemochromatosis gene product HFE in retinal pigment epithelium. *Invest Ophthalmol Vis Sci*. 2006;47(10):4238-44. doi: [10.1167/iops.06-0026](https://doi.org/10.1167/iops.06-0026) pmid: 17003411
23. Davies G, Dymock I, Harry J, Williams R. Deposition of melanin and iron in ocular structures in haemochromatosis. *Br J Ophthalmol*. 1972;56(4):338-42. doi: [10.1136/bjo.56.4.338](https://doi.org/10.1136/bjo.56.4.338) pmid: 5038719
24. Wolkow N, Song Y, Wu TD, Qian J, Guerquin-Kern JL, Dunaief JL. Aceruloplasminemia: retinal histopathologic manifestations and iron-mediated melanosome degradation. *Arch Ophthalmol*. 2011;129(11):1466-74. doi: [10.1001/archophthalmol.2011.309](https://doi.org/10.1001/archophthalmol.2011.309) pmid: 22084216
25. Dunaief JL. Iron induced oxidative damage as a potential factor in age-related macular degeneration: the Cogan Lecture. *Invest Ophthalmol Vis Sci*. 2006;47(11):4660-4. doi: [10.1167/iops.06-0568](https://doi.org/10.1167/iops.06-0568) pmid: 17065470
26. Ueda K, Kim HJ, Zhao J, Song Y, Dunaief JL, Sparrow JR. Iron promotes oxidative cell death caused by bisretinoids of retina. *Proc Natl Acad Sci U S A*. 2018;115(19):4963-4968. doi: [10.1073/pnas.1722601115](https://doi.org/10.1073/pnas.1722601115) pmid: 29686088
27. Kevany BM, Palczewski K. Phagocytosis of retinal rod and cone photoreceptors. *Physiology (Bethesda)*. 2010;25(1):8-15. doi: [10.1152/physiol.00038.2009](https://doi.org/10.1152/physiol.00038.2009) pmid: 20134024
28. Tripathy K, Salini B. Best Disease. 2023. In: StatPearls [Internet]. Treasure Island (FL): StatPearls Publishing; 2024-. pmid: 30725975
29. François J, De Rouck A, Fernandez-Sasso D. Electro-oculography in vitelliform degeneration of the macula. *Arch Ophthalmol*. 1967;77(6):726-33. doi: [10.1001/archophth.1967.00980020728003](https://doi.org/10.1001/archophth.1967.00980020728003) pmid: 6026180
30. Wood MJ, Skoien R, Powell LW. The global burden of iron overload. *Hepatol Int*. 2009;3(3):434-44. doi: [10.1007/s12072-009-9144-z](https://doi.org/10.1007/s12072-009-9144-z) pmid: 19669241
31. Plafker SM, O'Mealey GB, Szewda LI. Mechanisms for countering oxidative stress and damage in retinal pigment epithelium. *Int Rev Cell Mol Biol*. 2012;298:135-77. doi: [10.1016/B978-0-12-394309-5.00004-3](https://doi.org/10.1016/B978-0-12-394309-5.00004-3) pmid: 22878106
32. Lu L, Hackett SF, Mincey A, Lai H, Campochiaro PA. Effects of different types of oxidative stress in RPE cells. *J Cell Physiol*. 2006;206(1):119-25. doi: [10.1002/jcp.20439](https://doi.org/10.1002/jcp.20439) pmid: 15965958
33. Rogers BS, Symons RC, Komeima K, Shen J, Xiao W, Swaim ME, et al. Differential sensitivity of cones to iron-mediated oxidative damage. *Invest Ophthalmol Vis Sci*. 2007;48(1):438-45. doi: [10.1167/iops.06-0528](https://doi.org/10.1167/iops.06-0528) pmid: 17197565